Science of the Total Environment 645 (2018) 796–805

Contents lists available at ScienceDirect

Science of the Total Environment

journal homepage: www.elsevier.com/locate/scitotenv

Potential and environmental control of carbon sequestration in major ecosystems across arid and semi-arid regions in China

Qing Gu [a], Jin Wei [a], Shuchang Luo [a], Mingguo Ma [a], Xuguang Tang [a,b,*]

[a] Chongqing Engineering Research Center for Remote Sensing Big Data Application, School of Geographical Sciences, Southwest University, Chongqing 400715, China
[b] Institute of Geographic Sciences and Natural Resources Research, Chinese Academy of Sciences, Beijing 100101, China

HIGHLIGHTS

- Few attempts are made to systematically analyze carbon sequestration capacity of dryland ecosystems.
- All typical ecosystems acted as carbon sinks with varied magnitudes on an annual time scale.
- Distinct seasonality in carbon sequestration existed over dryland ecosystems except Gobi Desert.
- Water balance, instead of rainfall, is the primary environmental control for carbon sequestration.

GRAPHICAL ABSTRACT

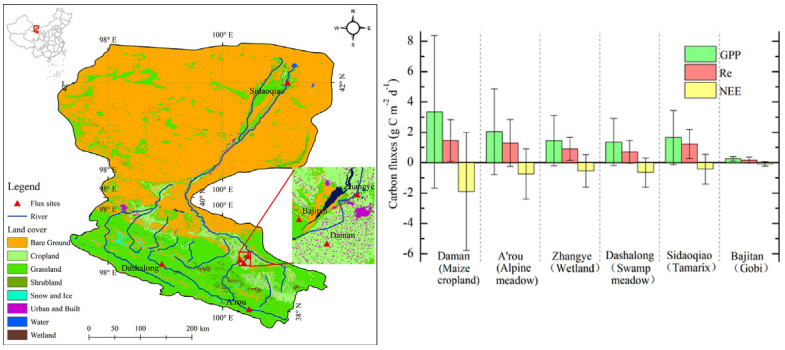

ARTICLE INFO

Article history:
Received 23 May 2018
Received in revised form 11 July 2018
Accepted 11 July 2018
Available online 19 July 2018

Editor: Elena PAOLETTI

Keywords:
Carbon flux
Arid and semi-arid area
Northwest China
Water balance
Climate change

ABSTRACT

With the continuous expansion of drylands in the context of global climate change, governments have implemented a series of greening policies such as afforestation, to reduce ecological degradation. However, owing to historical conditions and technical constraints, few attempts have been made to quantitatively assess the differences in carbon sequestration capacity and the associated environmental controls among major ecosystems in the arid and semi-arid areas. Based on six flux towers located in northwestern China measuring the carbon fluxes in a maize (*Zea mays* L.) cropland, alpine meadow, wetland, swamp meadow, Tamarix, and gobi desert, this work revealed that all ecosystems sequestered CO_2 at various magnitudes. The cropland had the highest carbon uptake, followed by the alpine meadow, swamp meadow, wetland and Tamarix, respectively. Distinct seasonal dynamics in carbon sequestration were observed across these ecosystems with the peak values in summertime, whereas the gobi desert exhibited as a weak carbon sink with considerable fluctuations around the year. In this water-limited region, soil water content instead of rainfall, is expected to be the primary environmental control on the land–atmosphere carbon fluxes, and regarded as a key linkage between hydrologic and ecologic processes. Therefore, not only the appropriate vegetation types, but also the water availability controlled by the local climatic constraints and soil characteristics, should be addressed in order to identify management strategies for ecological restoration in the dry areas.

© 2018 Elsevier B.V. All rights reserved.

1. Introduction

The terrestrial carbon budget represents the net CO_2 flux between the surface and the atmosphere during a specific period, which can

* Corresponding author at: Tiansheng Road No. 2, Beibei District, Chongqing 400715, China.
E-mail address: xgtang@swu.edu.cn (X. Tang).

https://doi.org/10.1016/j.scitotenv.2018.07.139
0048-9697/© 2018 Elsevier B.V. All rights reserved.

not only mitigate climate change through carbon absorption, but also accelerate climate warming through carbon release (Cox et al., 2000). Increased fossil fuel burning, cement production, uncontrolled deforestation and other anthropogenic activities since the industrial revolution have resulted in considerable increase in the emissions of CO_2, CH_4 and other greenhouse gases (Knox et al., 2015; Tang et al., 2017a). The atmospheric CO_2 concentration has increased by nearly 40% with 400 ppm (Betts et al., 2016). Moreover, the global-mean surface temperature is expected to rise by 1.5–4.5 °C by the middle of the 21st century, and precipitation may increase by 7–15% (Millar et al., 2017). These effects will significantly impact the carbon cycle of terrestrial ecosystems. Meanwhile, global climate warming will accelerate the snow melt and glacier thaw in polar and alpine regions, threatening the sustainable development of human society in the ecologically fragile areas (Yang et al., 2015; Liu et al., 2016a). Terrestrial ecosystems in the temperate and boreal regions are especially sensitive to climate change (Schlaepfer et al., 2017), which has attracted a great deal of attention from scientific community and international society in order to explore vegetation feedbacks to climate systems.

Arid and semi-arid ecosystems cover about 29.8% of the total surface area of the Earth (Wang et al., 2014). However, it is an indispensable part of terrestrial ecosystems and provides significant ecosystem services. Meanwhile, ecosystems in such regions are vulnerable to environmental changes because of insufficient rain, strong light and high water evaporation throughout the year (Nyantakyi-Frimpong and Bezner-Kerr, 2015). The responses of drylands to local climate mainly reflect in the distribution driven by water scarcity, community structure and functions which are controlled by ecohydrological interactions. Despite global drylands expanded by 4–8% over the past century, model projections revealed that the expansion would continue during the next century owing to frequent drought-inducing weather disasters (Milly and Dunne, 2016). The adverse consequences will threaten ecosystem services and influence human livelihoods through water scarcity, vegetation die-offs and land degradation (Reed et al., 2015). Through experimental observations and model simulations, the carbon sequestration capacity of terrestrial ecosystems on different time and space scales and their responses to the climatic changes have also been analyzed (Schimel et al., 2015). However, the ecological role of arid and semi-arid ecosystems to global carbon cycle has long been neglected.

As one of the highly sensitive areas around the world to climate variability, arid and semi-arid ecosystems covered a vast and continuous region in Northwest China (Xia et al., 2017). Currently, studies in the dry areas remain scarce until the integrated research network entitled “Heihe Watershed Allied Telemetry Experimental Research” (HiWATER) was implemented in China in May 2012 (Li et al., 2017). A series of flux towers across various ecosystems were installed from the upstream to downstream, and aimed to enhance the cognition of hydrological and biogeochemical processes, to build an international leading watershed observing system, and to manage limited water resources in the fragile environment by integrating multi-source data. Therefore, on the basis of measurements collected in 2014 from six flux tower sites in the typical ecosystems including maize (*Zea mays* L.) cropland, alpine meadow, wetland, swamp meadow, Tamarix and gobi desert, this study aimed to i) compare the magnitudes of the carbon sequestration capacity across various dryland ecosystems; ii) reveal the differences of seasonal dynamics in net carbon flux (NEE) and its two components–gross primary productivity (GPP) and ecosystem respiration (R_e) systematically; and iii) analyze the dominant environmental controls of different ecosystems in dry areas. Information on these aspects is vital to develop appropriate management measures for ecological restoration in the dry areas and to predict the potential effects of future trends of climatic changes.

2. Materials and methods

2.1. Study region

This study was conducted at the Heihe River Basin in the arid and semi-arid area of Northwest China (Fig. 1), the 2nd largest inland valley with an area of about 143,000 km^2 (Wu et al., 2017). This area is a temperate continental monsoon climate, with remarkable temperature differences among four seasons. Precipitation exhibits spatiotemporal heterogeneity affected by the geographic factors and atmospheric circulation. The distinct cold and arid landscapes in the basin from the upstream to downstream include alpine meadow, glaciers, desert, frozen soil, irrigated crops, forest, and riparian ecosystem (Li et al., 2017). In detail, the water source area is located in the upper reach, with obvious vertical zonation and abundant types of surface vegetation cover including alpine meadow, swamp, permafrost, snow and ice. The largest consumptive area lies in the middle reach of the basin with more than 91% of the population and more than 80% of the gross domestic product (GDP) in the region (Deng et al., 2015). Most of the land has been reclaimed as agricultural area.

2.2. Flux site description

The eddy covariance (EC) system has been widely used to measure the CO_2 and H_2O fluxes between a specific ecosystem and the atmosphere, which becomes a direct and effective method to examine the carbon budget of terrestrial ecosystems (Baldocchi, 2014). Based on the available carbon fluxes and meteorological data of typical vegetation types in the Heihe River Basin, this study selected six flux sites including Daman, A'rou, Zhangye, Dashalong, Sidaoqiao, Bajitan to represent various ecosystems. Key information and spatial distribution of these stations can be seen in Table 1 and Fig. 1.

The Daman superstation is located in the central oasis with a 40-m boundary layer tower constructed in September 2012. It is one of the artificial oasis experimental areas (irrigated cropland) in the midstream of the Heihe River Basin (Li et al., 2017). The annual total precipitation and mean temperature were 127.2 mm and 7.06 °C, respectively. In this region, corn is the typical crop type. The seeds are generally sown in the end of April, reach the maximum height of about 1.8 m during the summertime and then they are reaped in mid-September (Tang et al., 2017b). The A'rou superstation was installed in the end of 2012. It is situated in the upstream of the basin. A valley existed in the east-west direction with a maximum width (approximate 3 km) along north-south paths. The terrain around the A'rou site is generally flat despite of a small decline. Alpine meadow was the main vegetation in this area. Annual total precipitation and mean temperature were 484.8 mm and 0.85 °C, respectively.

The Zhangye wetland station is located in the middle of the Hexi Corridor, and data have been collected since June 2012. This site has an extraordinarily complex ecosystem including rivers, marshes, wet meadows and an arid irrigated cropland (Zhang et al., 2016). The Dashalong station lies in Qilian County of Qinghai Province with the high-cold swamp meadow distribution, and the EC system began to work in August 2013. The land cover at the site is alpine meadow, always covered by snow most of the time in the late autumn, winter, and early spring (Wang et al., 2017). The Sidaoqiao superstation is situated in the downstream of the Heihe River Basin. The flux tower is installed in Ejin Banner of Inner Mongolia, where a great number of Tamarix are distributed. Dataset of this site started from July 2013. The Bajitan gobi desert station has been operated since September 2012, which is situated in the middle reaches of the basin as well as the Daman and Zhangye wetland station (Liu et al., 2016b; Zeng et al., 2016).

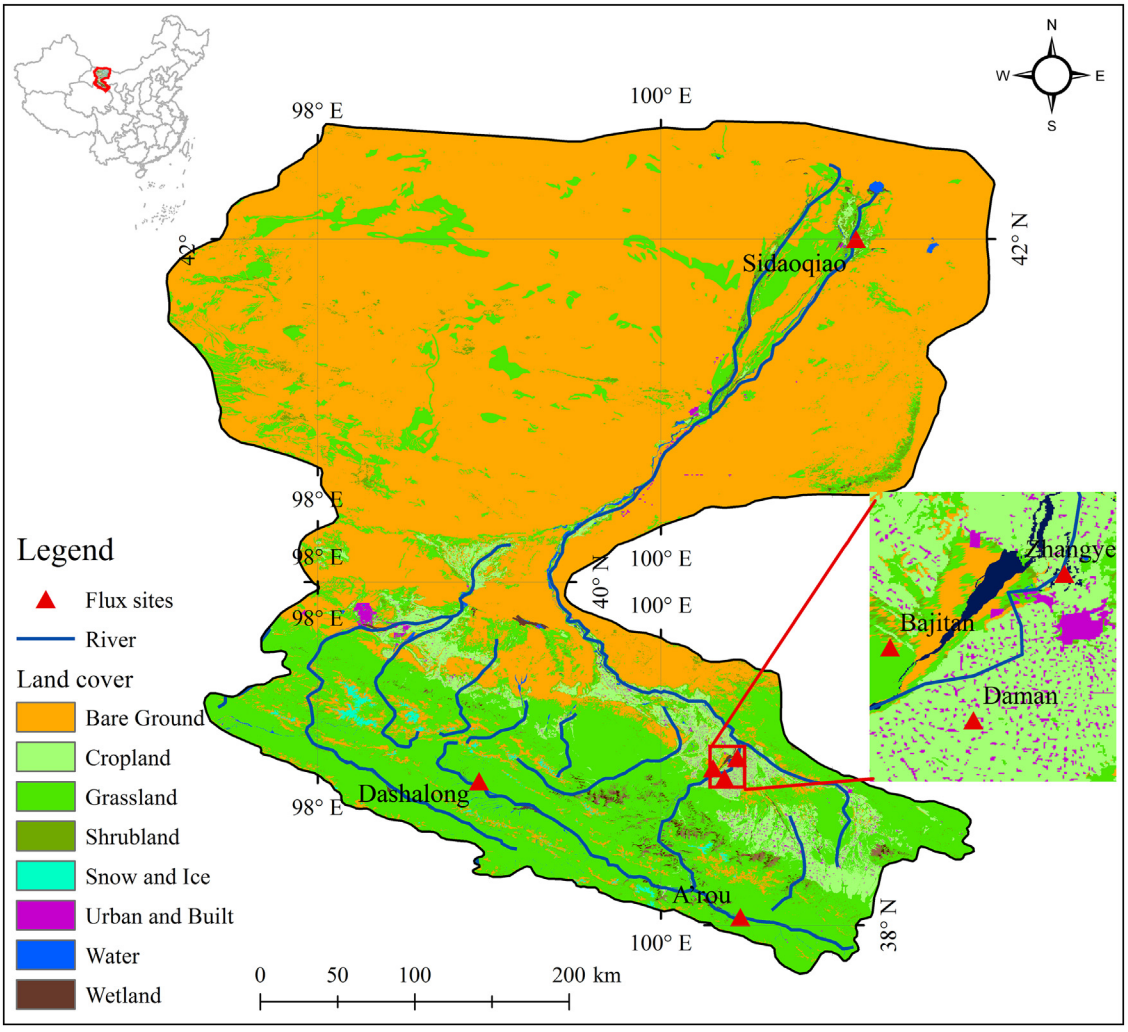

Fig. 1. Distribution of the six flux sites located in the arid and semi-arid region of Northwest China. The land cover classification data were produced by Department of Earth System Science: Tsinghua University, and can be downloaded from http://data.ess.tsinghua.edu.cn/data/.

2.3. Data acquisition and processing

To determine the differences in carbon sequestration and dominant environmental controls of different ecosystem types in the arid and semi-arid areas, this study collected continuous EC observations at the six flux sites during 2014 for comparison. Each of these sites has EC and automatic weather station (AWS) systems to measure ecosystem CO_2 and water fluxes, as well as the relevant weather conditions, including solar radiation (R_g), air and soil temperatures (T_a and T_s), relative humidity (RH), soil moisture profile (SWC), precipitation (P), and vapor pressure deficit (VPD). The observation heights were 4.5 m, 3.5 m, 5.2 m, 4.5 m, 8 m and 4.6 m for the Daman site, A'rou site, Zhangye site, Dashalong site, Sidaoqiao site and Bajitan site, respectively. The depths of instrument to measure soil temperature and moisture spanned from 2 cm, 4 cm, 10 cm, 20 cm, 40 cm and 100 cm except the wetland and swamp meadow owing to the special natural conditions.

The EC system is comprised of a three-dimensional sonic anemometer (CSAT3, Campbell Scientific, UT, USA) and a Li-7500A open path CO_2/H_2O gas analyzer (LI-COR Inc., NE, USA). Raw data from the EC sensor are continuously recorded at a frequency of 10 Hz. Observation data were processed using the EdiRe software (http://www.geos.ed.ac.uk/abs/research/micromet/EdiRe) developed by the University of Edinburgh, UK to half-hour flux dataset. The procedures included spike

Table 1
Characteristics of the six flux sites.

Sites	Longitude (°E)	Latitude (°N)	Altitude (m)	Vegetation type	Dominant specie	Mean temperature (°C)	Precipitation (mm)
Daman	100.3722	38.8555	1556	Maize cropland	*Zea mays* L.	7.06 ± 11.17	127.2
A'rou	100.4643	38.0473	3033	Alpine meadow	*Kobresia myosuroides*	0.85 ± 9.37	484.8
Zhangye	100.4464	38.9751	1460	Wetland	*Phragmites communis*	9.06 ± 10.55	119.9
Dashalong	98.9406	38.8399	3739	Swamp meadow	Nutgrass flatsedge	9.22 ± 8.55	324.8
Sidaoqiao	101.1374	42.0012	873	Tamarix	*Tamarix chinensis*	9.23 ± 13.10	24.8
Bajitan	100.3042	38.915	1562	Gobi	Reaumuria songarica	8.89 ± 10.37	104.3

Note: All these data were obtained through the data management and sharing platform of the Environmental and Ecological Science Data Center for West China (http://westdc.westgis.ac.cn/). The mean temperature and total precipitation represented the values during 2014 for each flux site. The standard deviations of mean temperature are also attached.

detection, two-dimensional coordinate rotation, lag correction of H_2O/CO_2 relative to the vertical wind component, sonic virtual temperature correction, density fluctuations (WPL correction) and frequency response correction (Goulden et al., 2006; Song et al., 2016). In addition to these processing steps, the half-hourly flux data were rejected in the following situations: i) when the sensor was malfunctioning (e.g., when a fault diagnostic signal occurred); ii) when precipitation happened within 1 h before and after the collection; iii) when the missing ratio was larger than 3% in the 30-min raw record; and iv) when the friction velocity was below 0.1 m s^{-1} at night (Liu et al., 2011, 2013).

Recently, these data have been released through the data management and sharing platform of the Environmental and Ecological Science Data Center for West China (http://westdc.westgis.ac.cn/), a part of China Flux Observation and Research Network (ChinaFLUX). However, owing to instrument malfunctions, power failure, and severe weather conditions, nearly 25% of the 1-year observation data are missing. The data gaps of the eddy covariance and meteorological data were filled using the similar method as Falge et al. (2001). In addition, the study considered the co-variation of fluxes with meteorological variables and the temporal auto-correlation of the fluxes (Reichstein et al., 2005). To obtain daily-, monthly- or annually-integrated values, a standardized gap-filling algorithm was developed. This study used the daytime-based flux partitioning method to partition NEE into its components GPP and R_e with the following equation (Lasslop et al., 2010; Tang et al., 2017b):

$$NEE = R_e - GPP$$

This approach applied a modified light-response curve based on the Lloyd and Taylor model (1994) to explain the sensitivity of R_e to temperature with the VPD limitation of GPP. The magnitudes of fluxes were calculated from daytime values, with only the parameters that define the temperature sensitivity of R_e needing to be inferred from night-time data. Therefore, the estimates of R_e based on the night-time measurements and GPP values estimated from the day-time observations were recognized as statistically independent. All of these works including gap-filling and flux partitioning were completed using the R-based package developed by the Max Planck Institute for Biogeochemistry (https://www.bgc-jena.mpg.de/REddyProc/brew/REddyProc.rhtml). These half-hour NEE, GPP, R_e and environmental variables are accumulated to daily and 8-day mean values to reflect the seasonal variations of terrestrial ecosystems.

In order to analyze the relationship between vegetation growth status and GPP, R_e and NEE, this study also calculated the normalized difference vegetation index (NDVI) using the site-level data from the MODIS BRDF/albedo product (Schaaf et al., 2002; Zhang et al., 2006). In particular, the nadir BRDF-adjusted reflectance daily L3 data (MCD43A4, V006) have removed view angle effects, and both cloud and aerosol contaminations were minimal. The MCD43A4 product provides the reflectance of MODIS bands 1–7 adjusted at a spatial resolution of 500 m by using the bidirectional reflectance distribution function to model the values from the nadir view (https://modis.ornl.gov/). The equation is as follows:

$$NDVI = {}^{NIR-R}/_{NIR+R}$$

where NIR and R represent the reflectance values of near-infrared (841–876 nm) and red (620–670 nm), respectively.

2.4. Statistical analyses

The annual mean values of GPP, R_e and NEE together with the associated standard deviations were calculated to compare the differences in magnitudes in various arid and semi-arid ecosystems. Then, Pearson correlation analysis was used to examine the environmental controls of the variability in carbon fluxes across these typical ecosystems using SPSS 19.0 (IBM, Chicago, IL, USA). Linear regressions were also performed to reveal the responses of GPP, R_e and NEE to the seasonal dynamics in NDVI on an 8-day period at the six flux sites.

3. Results

3.1. Differences in annual carbon fluxes among typical ecosystems

The annual mean carbon fluxes including GPP, R_e and NEE at the six flux sites in 2014 were shown in Table 2. Carbon fixation through vegetation photosynthesis was larger than carbon release by respiration in all dryland ecosystems, and terrestrial ecosystems in arid and semi-arid areas contribute to C sequestrations ranging from 29.2 g C m^{-2} y^{-1} to 690 g C m^{-2} y^{-1}. Even the gobi desert station in Bajitan exhibited a weak carbon sink of 29.2 g C m^{-2} y^{-1}, which is beneficial to the mitigation of local and regional climate change. However, both GPP and R_e at this site were extremely low because of sparse vegetation. Among all sites, the carbon sequestration capacity of maize cropland was the strongest with the largest GPP and R_e of 1223 g C m^{-2} y^{-1} and 533 g C m^{-2} y^{-1}, respectively. The potential carbon budget at the Daman superstation reached up to 690 g C m^{-2} y^{-1}, which was almost 2.5 times of carbon fixed at the A'rou alpine meadow (270.1 g C m^{-2} y^{-1}) and the Dashalong swamp meadow (237.3 g C m^{-2} y^{-1}) sites. Both GPP and R_e in the alpine meadow were apparently larger than that in the swamp meadow. Followed by the Zhangye wetland site, the net carbon flux was −197.1 g C m^{-2} y^{-1}. Although GPP was higher at the Sidaoqiao station by comparison with the Zhangye site, larger R_e offset more fixed CO_2, which resulted in a lower carbon sequestration in the Tamarix ecosystem.

The ratio of R_e to GPP at the six arid and semi-arid ecosystems were calculated to represent the efficiency of conversion of photosynthate to organic matter (Table 2). It revealed that the efficiency of the Daman cropland site was the largest with 0.56, and followed by the swamp meadow ecosystem at Dashalong station of 0.48. The carbon conversion efficiencies over the wetland, alpine meadow and gobi ecosystems were quite close, with no more than 0.4. The ratio of R_e to GPP was the highest in the Sidaoqiao Tamarix site, indicating that more CO_2 is released to the atmosphere through ecosystem respiration.

3.2. Seasonal patterns in GPP, R_e and NEE across various ecosystems

The seasonal dynamics of GPP, R_e and NEE at the six flux sites during 2014 were illustrated in Fig. 2. Except for the gobi ecosystem, the carbon sequestration and its two components showed in all sites a clear seasonal patterns over an 8-day period. The changing trends were quite consistent in spite of the magnitudes. More specifically, during the dormant seasons from late autumn to the next spring, GPP was nearly zero owing to lack of active photosynthetic activity. However, GPP began to increase rapidly with plant growth during the growing season, reached the peak at about week of year – WOY 25 in late July, and then gradually decreased with leaf withering. The duration of the atmospheric CO_2 uptake period lasted for approximately 140 days.

The seasonal dynamics in R_e generally co-varied with the variability in GPP despite of larger fluctuations around the one-year

Table 2
Annual mean GPP, R_e and NEE at the six arid and semi-arid flux sites during 2014.

Sites	Vegetation type	GPP	R_e	NEE	R_e/GPP
		g C m^{-2} d^{-1}			–
Daman	Maize cropland	3.35 ± 5.02	1.46 ± 1.38	−1.89 ± 3.89	0.44
A'rou	Alpine meadow	2.04 ± 2.83	1.30 ± 1.55	−0.74 ± 1.65	0.64
Zhangye	Wetland	1.45 ± 1.66	0.91 ± 0.76	−0.54 ± 1.07	0.63
Dashalong	Swamp meadow	1.36 ± 1.55	0.71 ± 0.76	−0.65 ± 0.96	0.52
Sidaoqiao	Tamarix	1.65 ± 1.79	1.23 ± 0.96	−0.42 ± 0.99	0.75
Bajitan	Gobi	0.25 ± 0.16	0.17 ± 0.20	−0.08 ± 0.15	0.68

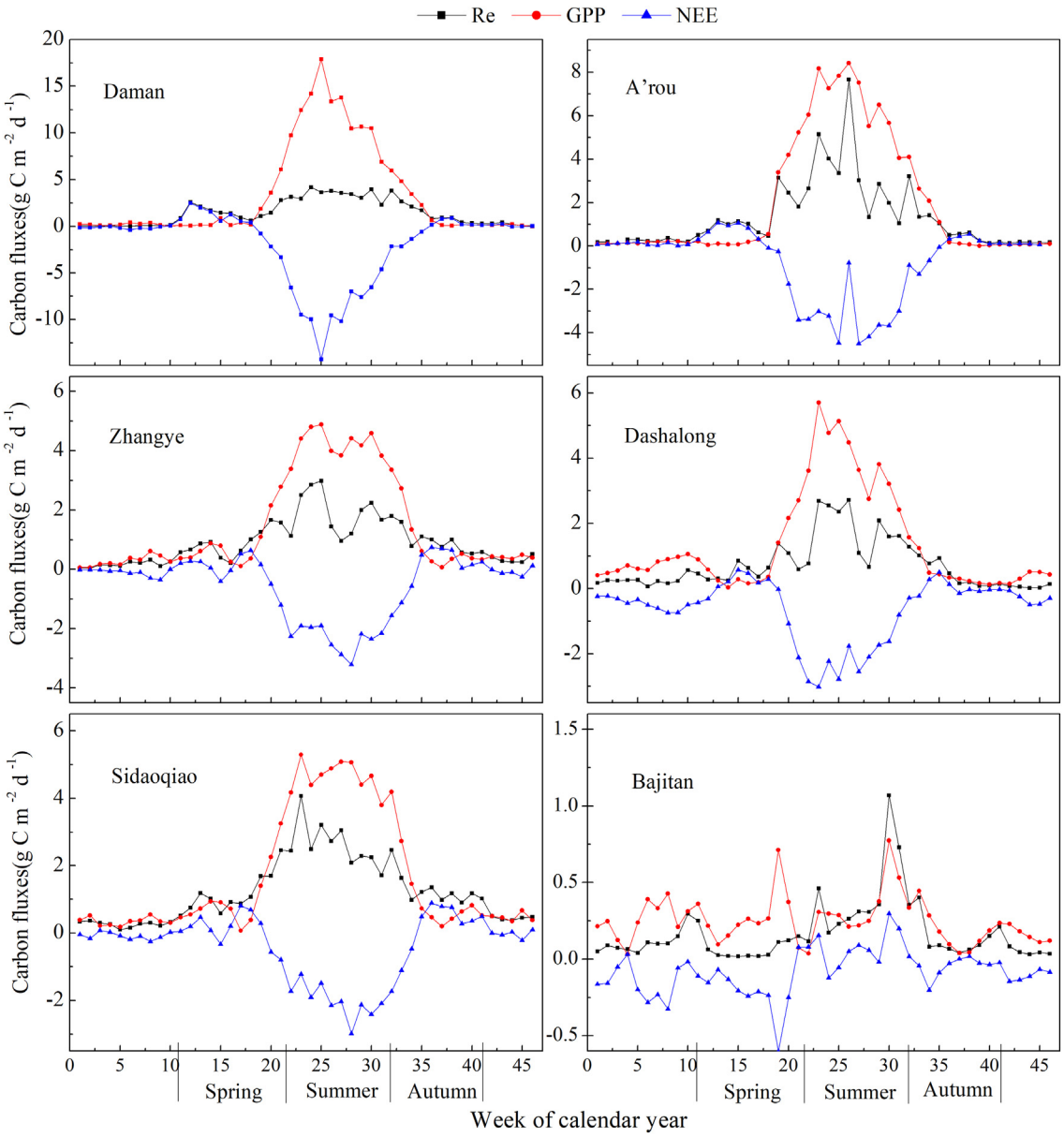

Fig. 2. Seasonal dynamics of gross primary production (GPP), ecosystem respiration (R_e) and net ecosystem carbon exchange (NEE) according to the plant functional types for these flux sites at the eight-day period. The associated information of each site can be found in Table 1.

measurements. It reached the peak values during the summertime at all sites. However, the peak period of R_e at the Bajtian station obviously lagged behind the other ecosystems. Moreover, R_e at all natural vegetation sites such as A'rou, Zhangye, Dashalong and Sidaoqiao decreased severely during specific periods in the growing season owing to high temperatures and water scarcity. Because of external water supply, R_e in the artificial oasis site – Daman maintained a high value during the growth period. In addition, R_e was apparently stronger than GPP during the transitions from dormant season to growth period. Compared with GPP and R_e, the seasonality of NEE functioned as a large valley in the growing season. NEE decreased rapidly with plant growth from WOY 18, reached the valley bottom around WOY 26, and then gradually increased until WOY 35. Both GPP and R_e fluctuated severely around the year at the Bajitan gobi site, but it acted as a weak carbon sink at the annual period.

This study also compared the seasonal carbon sequestration across six dryland ecosystems in accordance to the main growing seasons including spring, summer and autumn (Fig. 3). Springtime is the key phenological stage for leaf green-up. During this period, GPP were higher than R_e which led to positive net carbon assimilation at all these flux sites, especially for the Dashalong station. By contrast, except swamp meadow and gobi, almost all ecosystems at the Daman, A'rou, Zhangye and Sidaoqiao sites performed as carbon sources in autumn with a stronger R_e than GPP. Both GPP and R_e were active during the peak growth period. Therefore, summertime essentially determined the role of an ecosystem as a carbon source/sink. Among all ecosystems, the maize cropland sequestered the maximum C in summer. Interestingly, gobi Desert was neutral for carbon assimilation during this period, whereas spring and autumn significantly contributed to annual carbon sink.

3.3. Analysis of environmental controls

Pearson correlation analyses were conducted to explore the environmental restrictive factors of seasonal variations in GPP, R_e and NEE across these arid and semi-arid ecosystems (Table 3). Generally, the spatial distribution and species composition of various ecosystems are determined by local climatic conditions (Li et al., 2017). This study

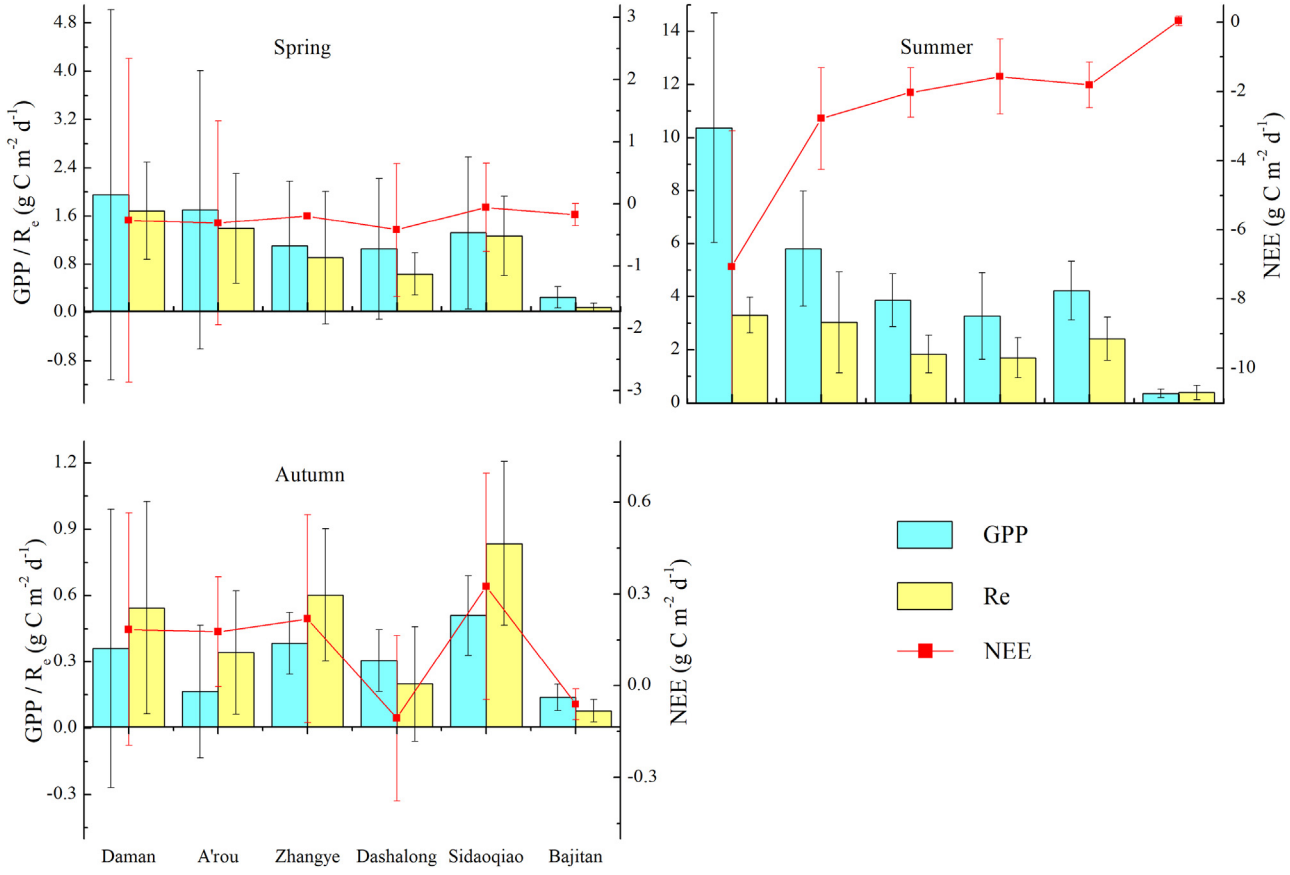

Fig. 3. Comparisons of seasonal mean GPP, R_e and NEE at the six flux sites during the periods of spring, summer and autumn, respectively. Error bars represent ±1 standard error.

revealed that nearly all environmental factors including light, heat and water were significantly and positively correlated to the GPP variability of vegetation ecosystems. As a key parameter affecting vegetation phenology, temperature is one of the most important factors controlling the carbon cycles. Particularly, T_s performed a closer correlation with GPP than T_a for most sites. Followed by R_g, it is the source of energy for vegetation photosynthesis. Although the amounts of natural rainfall (P) were not universally and significantly dominating the variations in GPP, soil water content (SWC) had a strong and positive correlation across cropland, meadow and Tamarix ecosystems. Meanwhile, the correlation analysis indicated that R_e was significantly influenced by temperature, VPD, R_g and SWC at the Daman, Zhangye and Sidaoqiao sites. However, nearly all climate factors were negatively correlated to R_e at the A'rou site, especially for the precipitation. The Dashalong meadow site had similar features in spite of weaker correlations. This study also found that at the gobi site, VPD and R_g mainly affected GPP,

Table 3
Correlation coefficients of the carbon fluxes (GPP, R_e and NEE) with the associated environmental factors over an 8-day period at the six flux sites.

Carbon fluxes (g C m^{-2} d^{-1})	Sites	R_g (W m^{-2})	VPD (h Pa)	Rh (%)	T_a (°C)	T_s (°C)	SWC (%)	P (mm)	NDVI
GPP	Daman	**0.609****	**0.425****	**0.479****	**0.683****	**0.694****	**0.715****	−0.080	**0.901****
	A'rou	**0.500****	**0.760****	**0.535****	**0.483****	**0.719****	**0.815****	**0.958****	**0.924****
	Zhangye	**0.597****	**0.578****	**0.450****	**0.726****	**0.769****	–	0.129	**0.941****
	Dashalong	**0.391****	**0.451****	**0.558****	**0.700****	**0.657****	–	0.086	**0.849****
	Sidaoqiao	**0.618****	**0.735****	0.211	**0.741****	**0.856****	**0.447****	**0.385****	**0.933****
	Bajitan	**0.398****	**0.406****	−0.163	0.311*	0.320*	0.123	−0.025	0.261
Re	Daman	**0.664****	**0.539****	**0.437****	**0.834****	**0.833****	**0.867****	−0.144	**0.847****
	A'rou	**−0.494****	**−0.636****	**0.452****	**−0.377****	−0.077	−0.562*	**−0.892****	**0.741****
	Zhangye	**0.658****	**0.669****	0.367*	**0.785****	**0.811****	–	0.175	**0.866****
	Dashalong	−0.225	−0.250	0.057	−0.202	−0.080	–	−0.212	**0.784****
	Sidaoqiao	**0.657****	**0.792****	0.165	**0.823****	**0.896****	**0.478****	**0.531****	**0.826****
	Bajitan	0.320*	0.352*	0.258	**0.446****	**0.452****	**0.549****	0.336*	**0.572****
NEE	Daman	**−0.550****	−0.357*	**−0.463****	**−0.587****	**−0.602****	**−0.616****	0.052	**−0.854****
	A'rou	**−0.486****	**−0.644****	**−0.493****	**−0.392****	**−0.774****	**−0.776****	**−0.909****	**−0.866****
	Zhangye	**−0.458****	**−0.421****	**−0.438****	**−0.569****	**−0.618****	–	−0.076	**−0.845****
	Dashalong	0.111	0.098	−0.149	−0.019	−0.137	–	0.146	**−0.755****
	Sidaoqiao	**−0.480****	**−0.560****	−0.221	**−0.541****	**−0.677****	−0.344*	−0.181	**−0.882****
	Bajitan	0.009	0.042	**0.508****	0.264	0.263	**0.596****	**0.468****	**0.491****

Note: ** and * mean that the correlation coefficients are significant at 0.01 and 0.05 level, respectively. Solar radiation–R_g (W m^{-2}), air temperature–T_a and soil temperature–T_s (°C), vapor pressure deficit–VPD (h Pa), relative humility–RH (%), soil water content–SWC (%) and precipitation–P (mm) are observed at these EC flux tower sites. T_s and SWC at the 10 cm depth were used. Time-series normalized difference vegetation index (NDVI) data were derived from the MCD43A4 product.

whereas R_e was majorly influenced by temperature and SWC. NEE represented the balance between GPP and Re. The correlation analysis implied that in the temperate continental monsoon climate zone, SWC was the dominant climate factor for carbon sequestration over all dryland ecosystems including gobi. The correlations reached up to −0.616 and −0.776 for the Daman cropland and A'rou alpine meadow, respectively. Followed by T_s, T_a, R_g and VPD, all these abiotic factors were positively correlated to net carbon assimilation.

As a proxy of vegetation response to complicated climate system, NDVI over all arid and semi-arid ecosystems exhibited a significant correlation with NEE (Table 3) for vegetation community, which directly reflected the biological control of terrestrial carbon cycling processes. Linear regression method was performed in the present study to further examine the response of ecosystem carbon fluxes (GPP, R_e and NEE) to the variability in NDVI on an 8-day period at the six flux sites. As shown in Fig. 4, both NEE and its two components were moderately and linearly correlated to NDVI with the high R^2 values except the Bajitan gobi site. In particular, the most significant relationship between NEE and NDVI was detected at the Sidaoqiao Tamarix ecosystem with R^2 of 0.80. This is compared with looking at the linear relationship with moderate R^2 values (approximately 0.70) for the A'rou, Daman and Zhangye sites. However, the variability in NEE at the Dashalong swamp meadow site fluctuated dramatically with the changes of NDVI. By comparison with the vegetation ecosystems, with the increase in NDVI, the net carbon assimilation at the Bajitan gobi site decreased instead, because more CO_2 released through ecosystem respiration than the carbon absorbed by photosynthesis.

4. Discussion and conclusion

4.1. Effect of climate conditions on carbon cycle in dryland ecosystems

Accurate evaluation of carbon budget in various ecosystems is crucial to our understanding of the global carbon balance (Tang et al., 2012; Baldocchi, 2014). Arid and semi-arid ecosystems are often overlooked in this regard because their spatially sparse vegetation cover and more fragile environmental conditions than those of other areas (Lioubimtseva and Henebry, 2009; Ahlström et al., 2015). However, understanding the potential and environmental controls of carbon sequestration over the dryland areas is vital in reducing the uncertainty in future climate projections given the large proportion in the area of global land surface.

Ultimately, the distribution and area of dryland ecosystems, as well as their structure, function and composition, are determined by the climate conditions (Schlaepfer et al., 2017). Although dry areas on the Earth are expected to expand in the coming decades, global temperature and precipitation forecasts vary latitudinally suggesting different overcomes for tropical, subtropical, and temperate drylands (Trenberth et al., 2014). Of particular concern for arid and semi-arid ecosystems, the frequency, intensity and duration of extreme weather events especially drought are predicted to become more severe than before (Schlesinger et al., 2016; Gou et al., 2017). It is noteworthy that climate warming under the influence of rising levels of atmospheric CO_2 concentration will exert substantial effects on hydrology and vegetation in snow or ice-dominated alpine regions (Barnett et al., 2005; Tague and

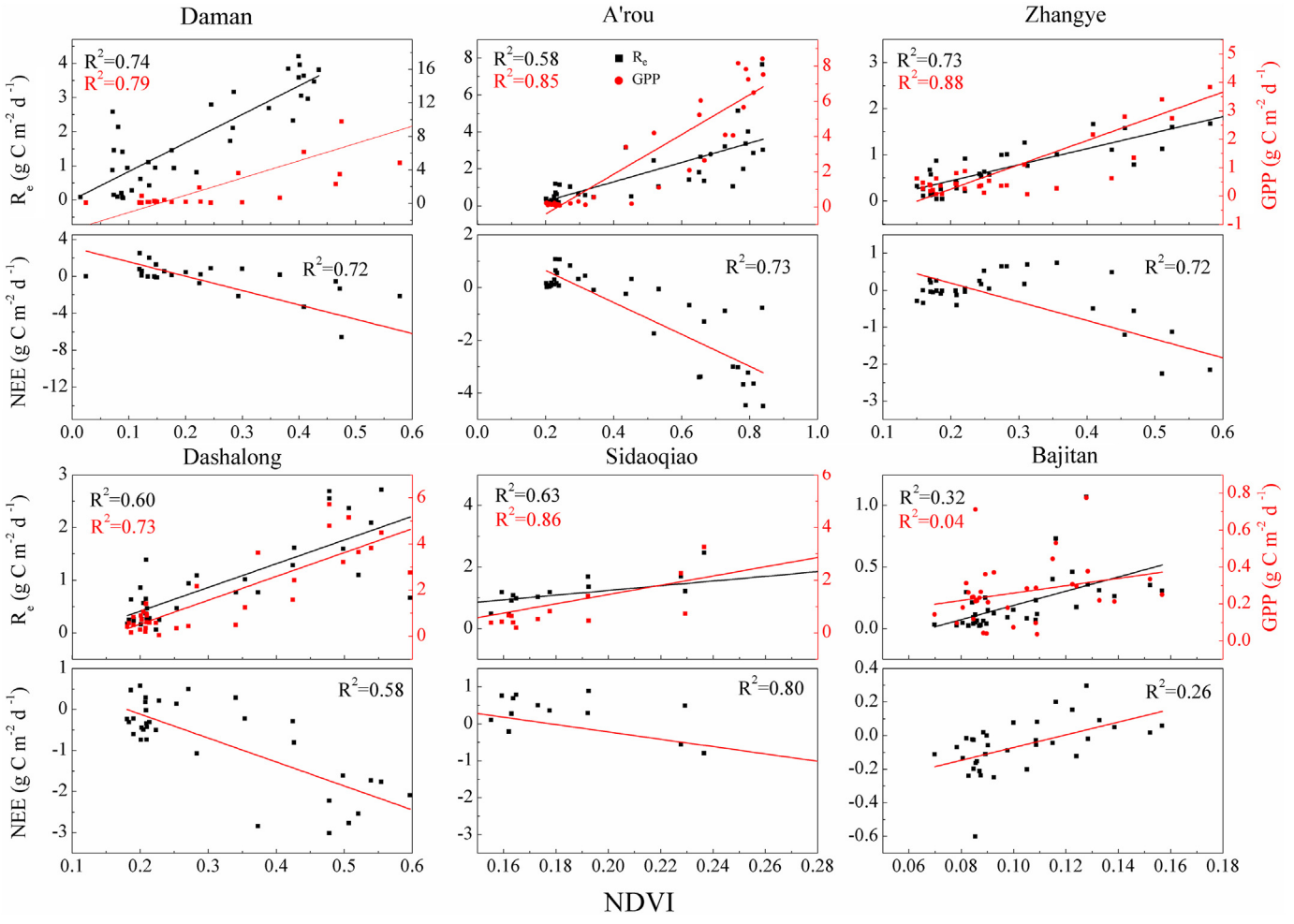

Fig. 4. Linear regression analysis of these carbon fluxes (GPP, R_e and NEE) with time-series normalized difference vegetation index (NDVI) on an eight-day period at the six flux sites.

Grant, 2009). In a warmer world, snow falls less in winter and the melting occurs earlier in spring. Even without any changes in precipitation intensity, both of these effects lead to a shift in peak of river runoff in winter and early spring, away from summer and autumn when the water demand is higher. Therefore, over the short time period, this could alter the water availability through ice/snow melting which is benefit for vegetation growth. However, the ecologically-fragile environment will become more at risk in a warming climate owing to scarce water supply after a long period. Meanwhile, climate change generally regulated the variation in vegetation phenology as well as annual NEE, which indicated that thermal condition at the onset of the growing season was critical for triggering the emergence of leaves (Marcolla et al., 2011). Previous studies indicated that early green-up could increase photosynthesis more than respiration among high-latitude biomes in the Northern Hemisphere (Kato et al., 2006; Piao et al., 2011). Potential outcomes include land use and cover changes, woody plant mortality and encroachment, and resistance of certain vegetation types. These vegetation responses vary among plant functional types and depend on seasonal and depth dynamics of soil moisture in addition to climate (Lauenroth et al., 2014). Therefore, more attentions are needed to reveal the vegetation responses to such events. Although this study indicated that the Bajitan site exhibited as a weak carbon sink with 29.2 g C m^{-2} y^{-1}, the expansion of gobi ecosystem will cause adverse consequences to the local carbon sequestration capacity.

In these regions, soil water content instead of rainfall, is the primary environmental control on the land-atmosphere carbon fluxes, and regarded as a key linkage between hydrologic and ecologic processes (Kurc and Small, 2007; Ahlström et al., 2015). Zhang et al. (2014) revealed that the mean carbon fixation of the northern China's grasslands was highly variable through years, ranging from 129 to 217 g C m^{-2} y^{-1} owing to the sensitivity to precipitation and droughts. Meanwhile, previous studies indicated that the carbon uptake was higher in meadow steppes and alpine meadows (Wang et al., 2010; Zhang et al., 2014), which was consistent with the observation in the A'rou site (270.1 g C m^{-2} y^{-1}) and Dashalong site (237.3 g C m^{-2} y^{-1}). However, because of the arid and semi-arid climate, the carbon sequestration of our region was relatively low by comparison with European temperate grasslands reaching up to 655 g C m^{-2} y^{-1} (Gilmanov et al., 2007). Jung et al. (2017) used empirical models to investigate the effect of changes in temperature and water availability on GPP, R_e and NEE at local and global scales, and found that water availability is the dominant factor of the local interannual variability in GPP and R_e. The present study also demonstrated that SWC played a more important role than P (Table 3). Natural rainfall is mainly evaporated to the atmosphere, whereas SWC is more directly relevant to the available water for plants. The scarcity of water availability is identified as the major element that reduces GPP by limiting photosynthetic rates, and shortening the length of the growing season (Rambal et al., 2014; Bernacchi and Vanloocke, 2015).

4.2. Management implications

A strong link existed between desertification of the drylands and emission of CO_2 from the land surface to the atmosphere (Lal, 2001). Desertification is defined as a biophysical process (soil, climate and vegetation status) driven by the socio-economic and environmental conditions, which involved accelerated soil erosion by wind and salinization, reduced soil quality and effective rooting depth, and decreased vegetation coverage and biomass productivity (Nosetto et al., 2006; Sousa et al., 2012; Ubugunov et al., 2017). However, the large global extension of arid and semi-arid ecosystems renders these areas a high potential to assimilate carbon. By means of six flux tower sites in the typical ecosystems in Northwest China, the drylands have been recognized as potential carbon sinks (Table 2) in spite of different magnitudes.

Grünzweig et al. (2003) firstly evaluated the annual carbon sequestration in an arid-land forest at the edge of the Negev Desert with 0.13–0.24 kg C m^{-2}. Similarly, this study revealed the CO_2 uptake from an afforestation system of Tamarix (Sidaoqiao site) with 153.3 g C m^{-2}. Hu et al. (2008) estimated the GPP of two grassland ecosystems in China including the alpine meadow steppe and the alpine swamp meadow. The annual GPP values were 495.54 g C m^{-2} and 423.7 g C m^{-2}, respectively, which were close to the results found in the A'rou and Dashalong sites. Meanwhile, we found that the carbon sequestration capacity of these arid and semi-arid ecosystems is generally lower by comparison with the wet areas. For instance, Jia et al. (2017) analyzed the carbon budget of the Liaohe Delta reed wetland in northern China with annual accumulation of 555.5 g C m^{-2}, which is much higher than the Zhangye wetland station with annual NEP of 197.1 g C m^{-2}. Owing to sufficient water provision as irrigated cropland at the Daman station, annual carbon uptake of maize reached to 690 g C m^{-2}, which was even more than that in the rainfed and irrigated maize cropland under no-till with about 510 g C m^{-2} (Verma et al., 2005). The existing crop residue of the previous year together with amount of rainfall during the non-growing season led to more carbon loss through microbial decomposition. Despite that the cultivated cropland can sequester more C than native vegetation, owing to the C removal by harvest as food for humans/livestock, harvest losses exceeded the carbon sequestration (NEE) by more than 60% (Kutsch et al., 2010; Smith et al., 2010). Thus, the real net biome production of cropland is not apparently higher than those in other ecosystems in the arid and semi-arid regions.

There is a consensus that the tropical regions contribute the most to the interannual variations in terrestrial carbon budget (Bousquet et al., 2000; Peylin et al., 2005, 2013). However, Poulter et al. (2014) suggested that the higher turnover rates of carbon pools in semi-arid biomes are an increasingly important factor for explaining the interannual dynamics in global carbon cycle and tropical rainforest may become less relevant drivers in the future. Gou et al. (2017) found that in terms of carbon sequestration potential, there is not a universally best restoration type for all climate zones. World grassland flux-tower synthesis estimated the mean net carbon uptake to be 191 g C m^{-2} y^{-1} for intensively managed grasslands and 70 g C m^{-2} y^{-1} for extensively managed grasslands (Gilmanov et al., 2010). The ecological restoration in the drylands is essentially constrained by the availability of water resource (Feng et al., 2013), whereas a dry and warm climate results in large deficits of water availability in a water-limited region. Gao et al. (2014) suggested that policies related to large-scale C sequestration initiatives under afforestation must first fully consider the status of water. Although the cultivated cropland from native steppe in semi-arid Inner Mongolia had a stronger ability to uptake carbon under optimal water condition, the steppe exhibited relatively stronger carbon uptake under drought stress and low temperature, which might be the result of evolutionary adaptations of steppe species to stressful environments (Zhang et al., 2007). Meanwhile, the conversions in the extensive dry regions have produced adverse ecological consequences at local and regional scales such as dust storms. In addition, soil carbon sequestration and land-use change are closely related (Post and Kwon, 2000; Upadhyay et al., 2006; Xiong et al., 2014). When natural vegetation is converted to cultivated crops, rapid declines in soil organic matter are due partly to a lower fraction of nonsoluble material in the more readily decomposed crop residues. But when agricultural land is no longer used for cultivation and allowed to revert to natural vegetation or replanted to perennial vegetation, soil organic carbon can accumulate. This accumulation process essentially reverses some of the effects responsible for soil organic carbon losses from when the land was converted from perennial vegetation. Apart from that, the C_4 species can better tolerate severe environmental stress and maintain intense photosynthesis during the growth season than C_3 species (Wang, 2002; Wittmer et al., 2010). Thus, the transformation of plant function types may be another strategy to adapt the dry areas. Given the high cost of human aided ecological restoration, it is therefore important to carefully choose the

appropriate restoration vegetation types according to the local climatic restraints to achieve best ecosystem services.

Currently, only a few flux sites in this area continuously measure the carbon flux between the biosphere and the atmosphere. Because of the limited data available using the EC technique, this study analyzed the differences in carbon sequestration and the main environmental controls among various arid and semi-arid ecosystems in 2014. However, the results could provide important scientific guidance for the ecological restoration in the dry areas. In line with the local conditions especially water availability, the expansion of afforestation efforts such as Tamarix into gobi desert, could contribute markedly to the C sequestration and associated benefits, such as restoration of degraded land, reduction in land surface runoff and soil desertification, and improvement of biodiversity.

Acknowledgments

This study was jointly supported by the National Natural Science Foundation of China (41701377), the Fundamental Research Funds for the Central Universities in China (SWU116088, XDJK2018C017), China Postdoctoral Science Foundation (2017M610109) and the National Undergraduate Training Programs for Innovation and Entrepreneurship of China (201710635007). This work used the flux data acquired from Heihe Watershed Allied Telemetry Experimental Research (Hi-WATER), a part of China Flux Observation and Research Network (ChinaFLUX). All technicians are acknowledged in site management and data collection. We also thank the principal contributors of the MODIS products, the Distributed Active Archive Center of the Oak Ridge National Laboratory and the Earth Observing System Data.

References

Ahlström, A., Raupach, M.R., Schurgers, G., Smith, B., Arneth, A., Jung, M., Reichstein, M., Canadell, J.G., Friedlingstein, P., Jain, A.K., Kato, E., Poulter, B., Sitch, S., Stocker, B.D., Viovy, N., Wang, Y.P., Wiltshire, A., Zaehle, S., Zeng, N., 2015. The dominant role of semi-arid ecosystems in the trend and variability of the land CO_2 sink. Science 348: 895–899. https://doi.org/10.1126/science.aaa1668.

Baldocchi, D., 2014. Measuring fluxes of trace gases and energy between ecosystems and the atmosphere - the state and future of the eddy covariance method. Glob. Chang. Biol. 20:3600–3609. https://doi.org/10.1111/gcb.12649.

Barnett, T.P., Adam, J.C., Lettenmaier, D.P., 2005. Potential impacts of a warming climate on water availability in snow-dominated regions. Nature 438:303–309. https://doi.org/10.1038/nature04141.

Bernacchi, C.J., Vanloocke, A., 2015. Terrestrial ecosystems in a changing environment: a dominant role for water. Annu. Rev. Plant Biol. 66:599–622. https://doi.org/10.1146/annurev-arplant-043014-114834.

Betts, R.A., Jones, C.D., Knight, J.R., Keeling, R.F., Kennedy, J.J., 2016. El Nino and a record CO_2 rise. Nat. Clim. Chang. 6:806–810. https://doi.org/10.1038/Nclimate3063.

Bousquet, P., Peylin, P., Ciais, P., Le Quere, C., Friedlingstein, P., Tans, P.P., 2000. Regional changes in carbon dioxide fluxes of land and oceans since 1980. Science 290: 1342–1346. https://doi.org/10.1126/science.290.5495.1342.

Cox, P.M., Betts, R.A., Jones, C.D., Spall, S.A., Totterdell, I.J., 2000. Acceleration of global warming due to carbon-cycle feedbacks in a coupled climate model. Nature 408: 184–187. https://doi.org/10.1038/35041539.

Deng, X.Z., Shi, Q.L., Zhang, Q., Shi, C.C., Yin, F., 2015. Impacts of land use and land cover changes on surface energy and water balance in the Heihe River Basin of China, 2000–2010. Phys. Chem. Earth 79-82:2–10. https://doi.org/10.1016/j.pce.2015.01.002.

Falge, E., Baldocchi, D., Olson, R., Anthoni, P., Aubinet, M., Bernhofer, C., Burba, G., Ceulemans, G., Clement, R., Dolman, H., Granier, A., Gross, P., Grunwald, T., Hollinger, D., Jensen, N.O., Katul, G., Keronen, P., Kowalski, A., Lai, C.T., Law, B.E., Meyers, T., Moncrieff, J., Moors, E., Munger, J.W., Pilegaard, K., Rannik, U., Rebmann, C., Suyker, A., Tenhunen, J., Tu, K., Verma, S., Vesala, T., Wilson, K., Wofsy, S., 2001. Gap filling strategies for long term energy flux data sets. Agric. For. Meteorol. 107:71–77. https://doi.org/10.1016/S0168-1923(00)00235-5.

Feng, X.M., Fu, B.J., Lu, N., Zeng, Y., Wu, B.F., 2013. How ecological restoration alters ecosystem services: an analysis of carbon sequestration in China's Loess Plateau. Sci. Rep.-UK 3. https://doi.org/10.1038/Srep02846.

Gao, Y., Zhu, X.J., Yu, G.R., He, N.P., Wang, Q.F., Tian, J., 2014. Water use efficiency threshold for terrestrial ecosystem carbon sequestration in China under afforestation. Agric. For. Meteorol. 195:32–37. https://doi.org/10.1016/j.agrformet.2014.04.010.

Gilmanov, T.G., Soussana, J.E., Aires, L., Allard, V., Ammann, C., Balzarolo, M., Barcza, Z., Bernhofer, C., Campbell, C.L., Cernusca, A., Cescatti, A., Clifton-Brown, J., Dirks, B.O.M., Dore, S., Eugster, W., Fuhrer, J., Gimeno, C., Gruenwald, T., Haszpra, L., Hensen, A., Ibrom, A., Jacobs, A.F.G., Jones, M.B., Lanigan, G., Laurila, T., Lohila, A., Manca, G., Marcolla, B., Nagy, Z., Pilegaard, K., Pinter, K., Pio, C., Raschi, A., Rogiers, N., Sanz, M.J., Stefani, P., Sutton, M., Tuba, Z., Valentini, R., Williams, M.L., Wohlfahrt, G., 2007. Partitioning European grassland net ecosystem CO_2 exchange into gross primary productivity and ecosystem respiration using light response function analysis. Agric. Ecosyst. Environ. 121:93–120. https://doi.org/10.1016/j.agee.2006.12.008.

Gilmanov, T.G., Aires, L., Barcza, Z., Baron, V.S., Belelli, L., Beringer, J., Billesbach, D., Bonal, D., Bradford, J., Ceschia, E., Cook, D., Corradi, C., Frank, A., Gianelle, D., Gimeno, C., Gruenwald, T., Guo, H.Q., Hanan, N., Haszpra, L., Heilman, J., Jacobs, A., Jones, M.B., Johnson, D.A., Kiely, G., Li, S.G., Magliulo, V., Moors, E., Nagy, Z., Nasyrov, M., Owensby, C., Pinter, K., Pio, C., Reichstein, M., Sanz, M.J., Scott, R., Soussana, J.F., Stoy, P.C., Svejcar, T., Tuba, Z., Zhou, G.S., 2010. Productivity, respiration, and light-response parameters of world grassland and agroecosystems derived from flux-tower measurements. Rangel. Ecol. Manag. 63:16–39. https://doi.org/10.2111/Rem-D-09-00072.1.

Gou, Q.Q., Wang, G.H., Qu, J.J., 2017. Variation in NEE and its response to environmental factors in an extremely arid desert wetland ecosystem. Contemp. Probl. Ecol. 10: 575–582. https://doi.org/10.1134/S1995425517050043.

Goulden, M.L., Winston, G.C., McMillan, A.M.S., Litvak, M.E., Read, E.L., Rocha, A.V., Elliot, J.R., 2006. An eddy covariance mesonet to measure the effect of forest age on land-atmosphere exchange. Glob. Chang. Biol. 12:2146–2162. https://doi.org/10.1111/j.1365-2486.2006.01251.x.

Grünzweig, J.M., Lin, T., Rotenberg, E., Schwartz, A., Yakir, D., 2003. Carbon sequestration in arid-land forest. Glob. Chang. Biol. 9:791–799. https://doi.org/10.1046/j.1365-2486.2003.00612.x.

Hu, Z.M., Yu, G.R., Fu, Y.L., Sun, X.M., Li, Y.N., Shi, P.L., Wangw, Y.F., Zheng, Z.M., 2008. Effects of vegetation control on ecosystem water use efficiency within and among four grassland ecosystems in China. Glob. Chang. Biol. 14:1609–1619. https://doi.org/10.1111/j.1365-2486.2008.01582.x.

Jia, Q.Y., Yu, W.Y., Zhou, L., Liang, C.H., 2017. Atmospheric and surface-condition effects on CO_2 exchange in the Liaohe delta wetland, China. WaterSA 9:806. https://doi.org/10.3390/W9100806.

Jung, M., Reichstein, M., Schwalm, C.R., Huntingford, C., Sitch, S., Ahlstrom, A., Arneth, A., Camps-Valls, G., Ciais, P., Friedlingstein, P., Gans, F., Ichii, K., Ain, A.K.J., Kato, E., Papale, D., Poulter, B., Raduly, B., Rodenbeck, C., Tramontana, G., Viovy, N., Wang, Y.P., Weber, U., Zaehle, S., Zeng, N., 2017. Compensatory water effects link yearly global land CO_2 sink changes to temperature. Nature 541 541-520. https://doi.org/10.1038/nature20780.

Kato, T., Tang, Y.H., Gu, S., Hirota, M., Du, M.Y., Li, Y.N., Zhao, X.Q., 2006. Temperature and biomass influences on interannual changes in CO_2 exchange in an alpine meadow on the Qinghai-Tibetan plateau. Glob. Chang. Biol. 12:1285–1298. https://doi.org/10.1111/j.1365-2486.2006.01153.x.

Knox, S.H., Sturtevant, C., Matthes, J.H., Koteen, L., Verfaillie, J., Baldocchi, D., 2015. Agricultural peatland restoration: effects of land-use change on greenhouse gas (CO_2 and CH_4) fluxes in the Sacramento-San Joaquin Delta. Glob. Chang. Biol. 21:750–765. https://doi.org/10.1111/gcb.12745.

Kurc, S.A., Small, E.E., 2007. Soil moisture variations and ecosystem-scale fluxes of water and carbon in semiarid grassland and shrubland. Water Resour. Res. 43. https://doi.org/10.1029/2006wr005011.

Kutsch, W.L., Aubinet, M., Buchmann, N., Smith, P., Osborne, B., Eugster, W., Wattenbach, M., Schrumpf, M., Schulze, E.D., Tomelleri, E., Ceschia, E., Bernhofer, C., Beziat, P., Carrara, A., Di Tommasi, P., Grunwald, T., Jones, M., Magliulo, V., Marloie, O., Moureaux, C., Olioso, A., Sanz, M.J., Saunders, M., Sogaard, H., Ziegler, W., 2010. The net biome production of full crop rotations in Europe. Agric. Ecosyst. Environ. 139:336–345. https://doi.org/10.1016/j.agee.2010.07.016.

Lal, R., 2001. Potential of desertification control to sequester carbon and mitigate the greenhouse effect. Clim. Chang. 51:35–72. https://doi.org/10.1023/A:1017529816140.

Lasslop, G., Reichstein, M., Papale, D., Richardson, A.D., Arneth, A., Barr, A., Stoy, P., Wohlfahrt, G., 2010. Separation of net ecosystem exchange into assimilation and respiration using a light response curve approach: critical issues and global evaluation. Glob. Chang. Biol. 16:187–208. https://doi.org/10.1111/j.1365-2486.2009.02041.x.

Lauenroth, W.K., Schlaepfer, D.R., Bradford, J.B., 2014. Ecohydrology of dry regions: storage versus pulse soil water dynamics. Ecosystems 17:1469–1479. https://doi.org/10.1007/s10021-014-9808-y.

Li, X., Liu, S.M., Xiao, Q., Ma, M.G., Jin, R., Che, T., Wang, W.Z., Hu, X.L., Xu, Z.W., Wen, J.G., Wang, L.X., 2017. Data descriptor: a multiscale dataset for understanding complex eco-hydrological processes in a heterogeneous oasis system. Sci. Data 4. https://doi.org/10.1038/Sdata.2017.83.

Lioubimtseva, E., Henebry, G.M., 2009. Climate and environmental change in arid Central Asia: impacts, vulnerability, and adaptations. J. Arid Environ. 73:963–977. https://doi.org/10.1016/j.jaridenv.2009.04.022.

Liu, S.M., Xu, Z.W., Wang, W.Z., Jia, Z.Z., Zhu, M.J., Bai, J., Wang, J.M., 2011. A comparison of eddy-covariance and large aperture scintillometer measurements with respect to the energy balance closure problem. Hydrol. Earth Syst. Sci. 15:1291–1306. https://doi.org/10.5194/hess-15-1291-2011.

Liu, S.M., Xu, Z.W., Zhu, Z.L., Jia, Z.Z., Zhu, M.J., 2013. Measurements of evapotranspiration from eddy-covariance systems and large aperture scintillometers in the Hai River Basin, China. J. Hydrol. 487:24–38. https://doi.org/10.1016/j.jhydrol.2013.02.025.

Liu, H.L., Willems, P., Bao, A.M., Wang, L., Chen, X., 2016a. Effect of climate change on the vulnerability of a socio-ecological system in an arid area. Glob. Planet. Chang. 137: 1–9. https://doi.org/10.1016/j.gloplacha.2015.12.014.

Liu, S.M., Xu, Z.W., Song, L.S., Zhao, Q.Y., Ge, Y., Xu, T.R., Ma, Y.F., Zhu, Z.L., Jia, Z.Z., Zhang, F., 2016b. Upscaling evapotranspiration measurements from multi-site to the satellite pixel scale over heterogeneous land surfaces. Agric. For. Meteorol. 230:97–113. https://doi.org/10.1016/j.agrformet.2016.04.008.

Marcolla, B., Cescatti, A., Manca, G., Zorer, R., Cavagna, M., Fiora, A., Gianelle, D., Rodeghiero, M., Sottocornola, M., Zampedri, R., 2011. Climatic controls and ecosystem

responses drive the inter-annual variability of the net ecosystem exchange of an alpine meadow. Agric. For. Meteorol. 151:1233–1243. https://doi.org/10.1016/j.agrformet.2011.04.015.
Millar, R.J., Fuglestvedt, J.S., Friedlingstein, P., Rogelj, J., Grubb, M.J., Matthews, H.D., Skeie, R.B., Forster, P.M., Frame, D.J., Allen, A.R., 2017. Emission budgets and pathways consistent with limiting warming to 1.5 degrees C. Nat. Geosci. 10:741–747. https://doi.org/10.1038/NGEO3031.
Milly, P.C.D., Dunne, K.A., 2016. Potential evapotranspiration and continental drying. Nat. Clim. Chang. 6:946–949. https://doi.org/10.1038/Nclimate3046.
Nosetto, M.D., Jobbagy, E.G., Paruelo, J.M., 2006. Carbon sequestration in semi-arid rangelands: comparison of Pinus ponderosa plantations and grazing exclusion in NW Patagonia. J. Arid Environ. 67:142–156. https://doi.org/10.1016/j.jaridenv.2005.12.008.
Nyantakyi-Frimpong, H., Bezner-Kerr, R., 2015. The relative importance of climate change in the context of multiple stressors in semi-arid Ghana. Glob. Environ. Chang. 32: 40–56. https://doi.org/10.1016/j.gloenvcha.2015.03.003.
Peylin, P., Bousquet, P., Le Quere, C., Sitch, S., Friedlingstein, P., McKinley, G., Gruber, N., Rayner, P., Ciais, P., 2005. Multiple constraints on regional CO_2 flux variations over land and oceans. Glob. Biogeochem. Cycles 19. https://doi.org/10.1029/2003gb002214.
Peylin, P., Law, R.M., Gurney, K.R., Chevallier, F., Jacobson, A.R., Maki, T., Niwa, Y., Patra, P.K., Peters, W., Rayner, P.J., Rodenbeck, C., van der Laan-Luijkx, I.T., Zhang, X., 2013. Global atmospheric carbon budget: results from an ensemble of atmospheric CO_2 inversions. Biogeosciences 10:6699–6720. https://doi.org/10.5194/bg-10-6699-2013.
Piao, S.L., Cui, M.D., Chen, A.P., Wang, X.H., Ciais, P., Liu, J., Tang, Y.H., 2011. Altitude and temperature dependence of change in the spring vegetation green-up date from 1982 to 2006 in the Qinghai-Xizang Plateau. Agric. For. Meteorol. 151:1599–1608. https://doi.org/10.1016/j.agrformet.2011.06.016.
Post, W.M., Kwon, K.C., 2000. Soil carbon sequestration and land-use change: processes and potential. Glob. Chang. Biol. 6:317–327. https://doi.org/10.1046/j.1365-2486.2000.00308.x.
Poulter, B., Frank, D., Ciais, P., Myneni, R.B., Andela, N., Bi, J., Broquet, G., Canadell, J.G., Chevallier, F., Liu, Y.Y., Running, S.W., Sitch, S., van der Werf, G.R., 2014. Contribution of semi-arid ecosystems to interannual variability of the global carbon cycle. Nature 509:600–603. https://doi.org/10.1038/nature13376.
Rambal, S., Lempereur, M., Limousin, J.M., Martin-StPaul, N.K., Ourcival, J.M., Rodriguez-Calcerrada, J., 2014. How drought severity constrains gross primary production (GPP) and its partitioning among carbon pools in a Quercus ilex coppice? Biogeosciences 11:6855–6869. https://doi.org/10.5194/bg-11-6855-2014.
Reed, M.S., Stringer, L.C., Dougill, A.J., Perkins, J.S., Atlhopheng, J.R., Mulale, K., Favretto, N., 2015. Reorienting land degradation towards sustainable land management: linking sustainable livelihoods with ecosystem services in rangeland systems. J. Environ. Manag. 151:472–485. https://doi.org/10.1016/j.jenvman.2014.11.010.
Reichstein, M., Falge, E., Baldocchi, D., Papale, D., Aubinet, M., Berbigier, P., Bernhofer, C., Buchmann, N., Gilmanov, T., Granier, A., Grunwald, T., Havrankova, K., Ilvesniemi, H., Janous, D., Knohl, A., Laurila, T., Lohila, A., Loustau, D., Matteucci, G., Meyers, T., Miglietta, F., Ourcival, J.M., Pumpanen, J., Rambal, S., Rotenberg, E., Sanz, M., Tenhunen, J., Seufert, G., Vaccari, F., Vesala, T., Yakir, D., Valentini, R., 2005. On the separation of net ecosystem exchange into assimilation and ecosystem respiration: review and improved algorithm. Glob. Chang. Biol. 11:1424–1439. https://doi.org/10.1111/j.1365-2486.2005.001002.x.
Schaaf, C.B., Gao, F., Strahler, A.H., Lucht, W., Li, X.W., Tsang, T., Strugnell, N.C., Zhang, X.Y., Jin, Y.F., Muller, J.P., Lewis, P., Barnsley, M., Hobson, P., Disney, M., Roberts, G., Dunderdale, M., Doll, C., D'Entremont, R.P., Hu, B.X., Liang, S.L., Privette, J.L., Roy, D., 2002. First operational BRDF, albedo nadir reflectance products from MODIS. Remote Sens. Environ. 83:135–148. https://doi.org/10.1016/S0034-4257(02)00091-3.
Schimel, D., Stephens, B.B., Fisher, J.B., 2015. Effect of increasing CO_2 on the terrestrial carbon cycle. Proc. Natl. Acad. Sci. U. S. A. 112:436–441. https://doi.org/10.1073/pnas.1407302112/-/DCSupplemental.
Schlaepfer, D.R., Bradford, J.B., Lauenroth, W.K., Munson, S.M., Tietjen, B., Hall, S.A., Wilson, S.D., Duniway, M.C., Jia, G., Pyke, D.A., Lkhagva, A., Jamiyansharav, K., 2017. Climate change reduces extent of temperate drylands and intensifies drought in deep soils. Nat. Commun. 8. https://doi.org/10.1038/Ncomms14196.
Schlesinger, W.H., Dietze, M.C., Jackson, R.B., Phillips, R.P., Rhoades, C.C., Rustad, L.E., Vose, J.M., 2016. Forest biogeochemistry in response to drought. Glob. Chang. Biol. 22: 2318–2328. https://doi.org/10.1111/gcb.13105.
Smith, P., Lanigan, G., Kutsch, W.L., Buchmann, N., Eugster, W., Aubinet, M., Ceschia, E., Beziat, P., Yeluripati, J.B., Osborne, B., Moors, E.J., Brut, A., Wattenbach, M., Saunders, M., Jones, M., 2010. Measurements necessary for assessing the net ecosystem carbon budget of croplands. Agric. Ecosyst. Environ. 139:302–315. https://doi.org/10.1016/j.agee.2010.04.004.
Song, Y., Jin, L., Zhu, G.F., Ma, M.G., 2016. Parameter estimation for a simple two-source evapotranspiration model using Bayesian inference and its application to remotely sensed estimations of latent heat flux at the regional scale. Agric. For. Meteorol. 230:20–32. https://doi.org/10.1016/j.agrformet.2016.03.019.
Sousa, F.P., Ferreira, T.O., Mendonca, E.S., Romero, R.E., Oliveira, J.G.B., 2012. Carbon and nitrogen in degraded Brazilian semi-arid soils undergoing desertification. Agric. Ecosyst. Environ. 148:11–21. https://doi.org/10.1016/j.agee.2011.11.009.
Tague, C., Grant, G.E., 2009. Groundwater dynamics mediate low-flow response to global warming in snow-dominated alpine regions. Water Resour. Res. 45. https://doi.org/10.1029/2008wr007179.
Tang, X.G., Wang, Z.M., Liu, D.W., Song, K.S., Jia, M.M., Dong, Z.Y., Munger, J.W., Hollinger, D.Y., Bolstad, P.V., Goldstein, A.H., Desai, A.R., Dragoni, D., Liu, X.P., 2012. Estimating the net ecosystem exchange for the major forests in the northern United States by integrating MODIS and AmeriFlux data. Agric. For. Meteorol. 156:75–84. https://doi.org/10.1016/j.agrformet.2012.01.003.
Tang, X., Li, H., Ma, M., Yao, L., Peichl, M., Arain, A., Goulden, M., 2017a. How do disturbances and climate effects on carbon and water fluxes differ between multi-aged and even-aged coniferous forests? Sci. Total Environ. 599:1583–1597. https://doi.org/10.1016/j.scitotenv.2017.05.119.
Tang, X.G., Ma, M.G., Ding, Z., Xu, X.B., Yao, L., Huang, X.J., Gu, Q., Song, L.S., 2017b. Remotely monitoring ecosystem water use efficiency of grassland and cropland in China's arid and semi-arid regions with MODIS data. Remote Sens. 9:616. https://doi.org/10.3390/Rs9060616.
Trenberth, K.E., Dai, A.G., van der Schrier, G., Jones, P.D., Barichivich, J., Briffa, K.R., Sheffield, J., 2014. Global warming and changes in drought. Nat. Clim. Chang. 4: 17–22. https://doi.org/10.1038/Nclimate2067.
Ubugunov, V.L., Gunin, P.D., Bazha, S.N., Drobyshev, Y.I., Ubugunova, V.I., 2017. Soil Desiccation as indicator of desertification of forest-steppe ecosystems in the Barguzin Depression. Arid. Ecosyst. 7:142–154. https://doi.org/10.1134/S2079096117030106.
Upadhyay, T.P., Solberg, B., Sankhayan, P.L., 2006. Use of models to analyse land-use changes, forest/soil degradation and carbon sequestration with special reference to Himalayan region: a review and analysis. Forest Policy Econ. 9:349–371. https://doi.org/10.1016/j.forpol.2005.10.003.
Verma, S.B., Dobermann, A., Cassman, K.G., Walters, D.T., Knops, J.M., Arkebauer, T.J., Suyker, A.E., Burba, G.G., Amos, B., Yang, H.S., Ginting, D., Hubbard, K.G., Gitelson, A.A., Walter-Shea, E.A., 2005. Annual carbon dioxide exchange in irrigated and rainfed maize-based agroecosystems. Agric. For. Meteorol. 131:77–96. https://doi.org/10.1016/j.agrformet.2005.05.003.
Wang, R.Z., 2002. The C_4 photosynthetic pathway and life forms in grassland species from North China. Photosynthetica 40:97–102. https://doi.org/10.1023/A:1020162728473.
Wang, Z., Xiao, X.M., Yan, X.D., 2010. Modeling gross primary production of maize cropland and degraded grassland in northeastern China. Agric. For. Meteorol. 150: 1160–1167. https://doi.org/10.1016/j.agrformet.2010.04.015.
Wang, C., Wang, X.B., Liu, D.W., Wu, H.H., Lu, X.T., Fang, Y.T., Cheng, W.X., Luo, W.T., Jiang, P., Shi, J.S., Yin, H.Q., Zhou, J.Z., Han, X.G., Bai, E., 2014. Aridity threshold in controlling ecosystem nitrogen cycling in arid and semi-arid grasslands. Nat. Commun. 5. https://doi.org/10.1038/Ncomms5799.
Wang, N., Jia, L., Zheng, C.L., Menenti, M., 2017. Estimation of subpixel snow sublimation from multispectral satellite observations. J. Appl. Remote. Sens. 11. https://doi.org/10.1117/1.Jrs.11.046017.
Wittmer, M.H.O.M., Auerswald, K., Bai, Y.F., Schaufele, R., Schnyder, H., 2010. Changes in the abundance of C_3/C_4 species of Inner Mongolia grassland: evidence from isotopic composition of soil and vegetation. Glob. Chang. Biol. 16:605–616. https://doi.org/10.1111/j.1365-2486.2009.02033.x.
Wu, F., Bai, Y.P., Zhang, Y.L., Li, Z.H., 2017. Balancing water demand for the Heihe River basin in Northwest China. Phys. Chem. Earth 101:178–184. https://doi.org/10.1016/j.pce.2017.07.002.
Xia, J., Ning, L., Wang, Q., Chen, J.X., Wan, L., Hong, S., 2017. Vulnerability of and risk to water resources in arid and semi-arid regions of West China under a scenario of climate change. Clim. Chang. 144:549–563. https://doi.org/10.1007/s10584-016-1709-y.
Xiong, X., Grunwald, S., Myers, D.B., Ross, C.W., Harris, W.G., Comerford, N.B., 2014. Interaction effects of climate and land use/land cover change on soil organic carbon sequestration. Sci. Total Environ. 493:974–982. https://doi.org/10.1016/j.scitotenv.2014.06.088.
Yang, H., Andersen, T., Dörsch, P., Tominaga, K., Thrane, J.-E., Hessen, D.O., 2015. Greenhouse gas metabolism in Nordic boreal lakes. Biogeochemistry 126:211–225. https://doi.org/10.1007/s10533-015-0154-8.
Zeng, Y.J., Xie, Z.H., Yu, Y., Liu, S., Wang, L.Y., Jia, B.H., Qin, P.H., Chen, Y.N., 2016. Ecohydrological effects of stream-aquifer water interaction: a case study of the Heihe River basin, northwestern China. Hydrol. Earth Syst. Sci. 20:2333–2352. https://doi.org/10.5194/hess-20-2333-2016.
Zhang, X.Y., Friedl, M.A., Schaaf, C.B., 2006. Global vegetation phenology from Moderate Resolution Imaging Spectroradiometer (MODIS): evaluation of global patterns and comparison with in situ measurements. J. Geophys. Res. Biogeosci. 111. https://doi.org/10.1029/2006jg000217.
Zhang, W.L., Chen, S.P., Chen, J., Wei, L., Han, X.G., Lin, G.H., 2007. Biophysical regulations of carbon fluxes of a steppe and a cultivated cropland in semiarid Inner Mongolia. Agric. For. Meteorol. 146:216–229. https://doi.org/10.1016/j.agrformet.2007.06.002.
Zhang, L., Guo, H.D., Jia, G.S., Wylie, B., Gilmanov, T., Howard, D., Ji, L., Xiao, J.F., Li, J., Yuan, W.P., Zhao, T.B., Chen, S.P., Zhou, G.S., Kato, T., 2014. Net ecosystem productivity of temperate grasslands in northern China: an upscaling study. Agric. For. Meteorol. 184:71–81. https://doi.org/10.1016/j.agrformet.2013.09.004.
Zhang, Q., Sun, R., Jiang, G.Q., Xu, Z.W., Liu, S.M., 2016. Carbon and energy flux from a Phragmites australis wetland in Zhangye oasis-desert area, China. Agric. For. Meteorol. 230:45–57. https://doi.org/10.1016/j.agrformet.2016.02.019.